Data report: $^{87}Sr/^{86}Sr$ in pore fluids from NanTroSEIZE Expeditions 322 and 333[1]

Craig Joseph,[2] Marta E. Torres,[2] and Brian Haley[2]

Chapter contents

[1] Joseph, C., Torres, M.E., and Haley, B., 2013. Data report: $^{87}Sr/^{86}Sr$ in pore fluids from NanTroSEIZE Expeditions 322 and 333. *In* Saito, S., Underwood, M.B., Kubo, Y., and the Expedition 322 Scientists, *Proc. IODP,* 322: Tokyo (Integrated Ocean Drilling Program Management International, Inc.). doi:10.2204/iodp.proc.322.207.2013
[2] College of Earth, Ocean and Atmospheric Science, 104 CEOAS Administration Building, Oregon State University, Corvallis OR 97331, USA. Correspondence author: mtorres@coas.oregonstate.edu

Abstract

We report on the Sr isotopic composition of pore fluids recovered during Integrated Ocean Drilling Program Expeditions 322 and 333 at Sites C0011 and C0012, drilled on the Philippine Sea plate before subduction along the Nankai Trough. Acidified pore fluids were directly loaded into EICHROM Sr-specific columns, and isotopic analysis was performed using a Nu multicollector inductively coupled mass spectrometer. At both Sites C0011 and C0012, $^{87}Sr/^{86}Sr$ decreases with depth from the seawater value to ~0.7069 at a depth that corresponds to the bottom of lithologic Unit I, which consists of ash-bearing hemipelagic sediments. This decrease is consistent with the reported observation of increasing ash alteration with depth within Subunit IB. Pore fluids recovered from lithologic Units II–IV show a relatively constant $^{87}Sr/^{86}Sr$ ratio, which ranges between 0.7069 and 0.7065 at both sites. The volcaniclastic turbidites of Unit V and the red clay (Unit IV) directly overlying the basement were only recovered at Site C0012. The $^{87}Sr/^{86}Sr$ ratio below Unit IV shows a marked decrease, reaching the lowest value of 0.704367 in the deepest pore fluids recovered (529 m below seafloor), suggesting a diffusional communication with an ^{87}Sr-depleted fluid in the igneous upper crust.

Introduction

The Nankai Trough Seismogenic Zone Experiment (NanTroSEIZE) was designed to constrain in situ properties at seismogenic depths in an effort to understand fault zone behavior during earthquake nucleation and rupture propagation (Tobin and Kinoshita, 2006). Two sites were drilled during Integrated Ocean Drilling Program (IODP) Expeditions 322 and 333 on the subducting Philippine Sea plate to characterize the subducting materials before deformation. Site C0011, located on the northeast flank of a prominent bathymetric high (Kashinosaki Knoll), targeted a 1050 m sediment column (based on the seismic profile), of which we were able to recover 858 m. This section consists of sandy turbidite intervals within hemipelagic sediment (Figs. **F1, F2**). Site C0012 targeted a 526 m sedimentary section near the crest of the Kashinosaki Knoll (Fig. **F1**). Coring penetrated 23 m into igneous basement at 630.5 meters below seafloor (mbsf) (see the **"Expedition 322 summary"** chapter [Underwood et al., 2010]; Expedition 333 Scientists, 2012).

doi:10.2204/iodp.proc.322.207.2013

A fundamental component of our understanding of subduction inputs focuses on sampling sediments, fluids, and crustal rocks because fluids and associated diagenetic reactions affect hydrological parameters (e.g., permeability and pore pressure) and may regulate the mechanical state of the plate interface at depth. The isotopic composition of strontium (Sr) acts as a conservative tracer that does not undergo biological fractionation (Mook, 2001). Because of this property, $^{87}Sr/^{86}Sr$ has proved to be valuable in establishing fluid-rock reactions, sources, and fluid mixing (e.g., Torres et al., 2004; Teichert et al., 2005; Solomon et al., 2009; Joseph et al., 2012). Potential source materials responsible for the $^{87}Sr/^{86}Sr$ of interstitial waters in this region are continental detritus ($^{87}Sr/^{86}Sr$ ~ 0.7119–0.7133), biogenic calcite ($^{87}Sr/^{86}Sr$ ~ 0.7075–0.7092), volcanic ash ($^{87}Sr/^{86}Sr$ ~ 0.706), and oceanic crust ($^{87}Sr/^{86}Sr$ ~ 0.703) (Veizer, 1989). Here we report on the $^{87}Sr/^{86}Sr$ composition of fluids sampled from the sediment column prior to subduction.

Analytical methods

The isotopic composition of Sr was measured in pore fluid samples recovered from Sites C0011 and C0012. Pore fluids were directly loaded into the separation columns after acidification. Sr separation was carried out using a 50 µL Sr-specific column and resin from EICHROM. Isotopic analysis of a solution containing 300 ng Sr was performed using the Nu Plasma multicollector inductively coupled mass spectrometer (MC-ICPMS) housed in the W.M. Keck Collaboratory for Plasma Spectrometry in the College of Oceanic and Atmospheric Science at Oregon State University (OSU-COAS; USA). $^{87}Sr/^{86}Sr$ data were normalized to National Bureau of Standards standard NBS 987, with a reported $^{87}Sr/^{86}Sr$ value of 0.710245. A mean value of 0.710225 ± 0.000052 (2σ mean; n = 91) was obtained for repeated measurements. Replicate analysis of an in-house standard yielded a $^{87}Sr/^{86}Sr$ ratio of 0.708170 ± 0.000051 (2σ mean; n = 79).

Results and discussion

A total of 65 pore fluid samples were analyzed, and the data are listed in Table **T1.** Figure **F2** shows the downcore $^{87}Sr/^{86}Sr$ depth profiles in the context of the corresponding lithology. At Site C0011, the shallowest sampled analyzed (Section 333-C0011D-1H-4; 24.98 mbsf) has an $^{87}Sr/^{86}Sr$ ratio of 0.708710, which is markedly lower than the seawater value of 0.70917, as shown by the red rectangle on the x-axis (Fig. **F2**). Sr isotopic ratios continue to decrease with depth to ~350 mbsf, which coincides with the boundary between the hemipelagic pyroclastic sediments of lithologic Unit I and the volcanic turbidites of Unit II and is denoted by a horizontal arrow marked "A" (Fig. **F2**). The $^{87}Sr/^{86}Sr$ ratio in pore fluids recovered from Unit II–IV sediments shows little variability, with values ranging between 7.06504 and 0.706916, except for the two deepest samples analyzed (850.44 and 858.34 mbsf), which have values of 0.706991 and 0.707298. A mixing diagram showing the $^{87}Sr/^{86}Sr$ ratio from Site C0011 versus the inverse of the Sr concentration measured onboard indicates a two-end-member system characterized by fluid mixing between seawater ($^{87}Sr/^{86}Sr$ = 0.70917) and an evolved, ^{87}Sr-depleted fluid ($^{87}Sr/^{86}Sr$ = 0.70650) (Fig. **F3**). The ^{87}Sr-depleted fluid likely results from alteration of the volcanic ash layers in lithologic Subunit IA (Fig. **F2**). It is worth noting that the shipboard sedimentologists from Expedition 333 reported that the ash recovered within Subunit IA shows little evidence for alteration, whereas the severity of ash alteration increases with depth below the transition from Subunit IA to IB at ~252 mbsf (Fig. **F2**) (Expedition 333 Scientists, 2012). The tuffaceous sandstones of Unit II (348–578 mbsf; Fig. **F2**) may also have contributed to the ^{87}Sr-depleted fluids at this site; however, smear slide observations revealed mostly unaltered glass within Unit II sediments (Expedition 333 Scientists, 2012). Unfortunately, because of technical drilling difficulties the hole was aborted before reaching the target basement depth. Because of this, the deepest sediments at this site, which may have shown a diffusional communication with a more evolved fluid in the upper crust, were not recovered.

The shallowest sample analyzed at Site C0012 (Section 322-C0012A-5R-2) is also highly depleted in ^{87}Sr relative to seawater, with an $^{87}Sr/^{86}Sr$ ratio of 0.707640. Similar to observations at Site C0011, the Sr isotopic ratio continues to decrease with depth toward the bottom of lithologic Unit I (denoted by the blue arrow "A" in Fig. **F2**), reaching a value of 0.706884 at ~144 mbsf. This lithologic unit is characterized by the presence of abundant ash layers. The potential contribution of ash to $^{87}Sr/^{86}Sr$ in the upper 150 mbsf at this site is also apparent in the mixing diagram in Figure **F3.** Consistent with observations at Site C0011, the Sr isotopic ratio of fluids recovered from lithologic Units II–IV remains relatively constant, with $^{87}Sr/^{86}Sr$ values ranging from 0.706884 to 0.706502 (Fig. **F2**). Deeper in the formation, the fluids recovered from Units V and VI show a marked decrease in the Sr isotope ratios, which reach a mini-

mum $^{87}Sr/^{86}Sr$ value of 0.70436 at 529 mbsf, indicative of fluids modified by reaction with the underlying oceanic crust ($^{87}Sr/^{86}Sr$ ~ 0.7030) (Fig. F3).

Acknowledgments

This research used samples and data provided by the Integrated Ocean Drilling Program (IODP), which is sponsored by the US National Science Foundation and participating countries under management of IODP Management International, Inc. (IODP-MI). We gratefully acknowledge the efforts of the D/V *Chikyu* shipboard and drilling personnel and of the Scientific Parties of IODP Expeditions 322 and 333. Funding for this research was provided by the US Science Support Program (USSP) and through the National Science Foundation OCE-1029981 grant.

References

Expedition 333 Scientists, 2012. Expedition 333 summary. *In* Henry, P., Kanamatsu, T., Moe, K., and the Expedition 333 Scientists, *Proc. IODP,* 333: Tokyo (Integrated Ocean Drilling Program Management International, Inc.). **doi:10.2204/iodp.proc.333.101.2012**

Joseph, C., Torres, M.E., Martin, R.A., Haley, B.A., Pohlman, J.W., Riedel, M., and Rose, K., 2012. Using the $^{87}Sr/^{86}Sr$ of modern and paleoseep carbonates from northern Cascadia to link modern fluid flow to the past. *Chem. Geol.,* 334:122–130. **doi:10.1016/j.chemgeo.2012.10.020**

Mook, W.G., 2001. Applications to low temperature systems. *In* Geyh, M. (Ed.), *Environmental Isotopes in the Hydrological Cycle: Principles and Applications* (Vol. 4): *Groundwater: Saturated and Unsaturated Zone:* Vienna (Int. At. Energy Agency), 49–118. **http://www-naweb.iaea.org/napc/ih/documents/global_cycle/vol%20IV/IV_Ch5.pdf**

Solomon, E.A., Kastner, M., Wheat, C.G., Jannasch, H., Robertson, G., Davis, E.E., and Morris, J.D., 2009. Long-term hydrogeochemical records in the oceanic basement and forearc prism at the Costa Rica subduction zone. *Earth Planet. Sci. Lett.,* 282(1–4):240–251. **doi:10.1016/j.epsl.2009.03.022**

Teichert, B.M.A., Torres, M.E., Bohrmann, G., and Eisenhauer, A., 2005. Fluid sources, fluid pathways and diagenetic reactions across an accretionary prism revealed by Sr and B geochemistry. *Earth Planet. Sci. Lett.,* 239(1–2):106–121. **doi:10.1016/j.epsl.2005.08.002**

Tobin, H.J., and Kinoshita, M., 2006. Investigations of seismogenesis at the Nankai Trough, Japan. *IODP Sci. Prosp.,* NanTroSEIZE Stage 1. **doi:10.2204/iodp.sp.nantroseize1.2006**

Torres, M.E., Teichert, B.M.A., Tréhu, A.M., Borowski, W., and Tomaru, H., 2004. Relationship of pore water freshening to accretionary processes in the Cascadia margin: fluid sources and gas hydrate abundance. *Geophys. Res. Lett.,* 31:L22305. **doi:10.1029/2004GL021219**

Underwood, M.B., Saito, S., Kubo, Y., and the Expedition 322 Scientists, 2010. Expedition 322 summary. *In* Saito, S., Underwood, M.B., Kubo, Y., and the Expedition 322 Scientists, *Proc. IODP,* 322: Tokyo (Integrated Ocean Drilling Program Management International, Inc.). **doi:10.2204/iodp.proc.322.101.2010**

Veizer, J., 1989. Strontium isotopes in seawater through time. *Annu. Rev. Earth Planet. Sci.,* 17(1):141–167. **doi:10.1146/annurev.ea.17.050189.001041**

Initial receipt: 29 June 2012
Acceptance: 4 February 2013
Publication: 21 May 2013
MS 322-207

Figure F1. A. Bathymetric map showing locations of Sites C0011 and C0012 on the incoming Philippine Sea plate. **B.** Seismic reflection Line 95 showing Sites C0011 and C0012. VE = vertical exaggeration. (From the "Expedition 322 summary" chapter [Underwood et al., 2010].)

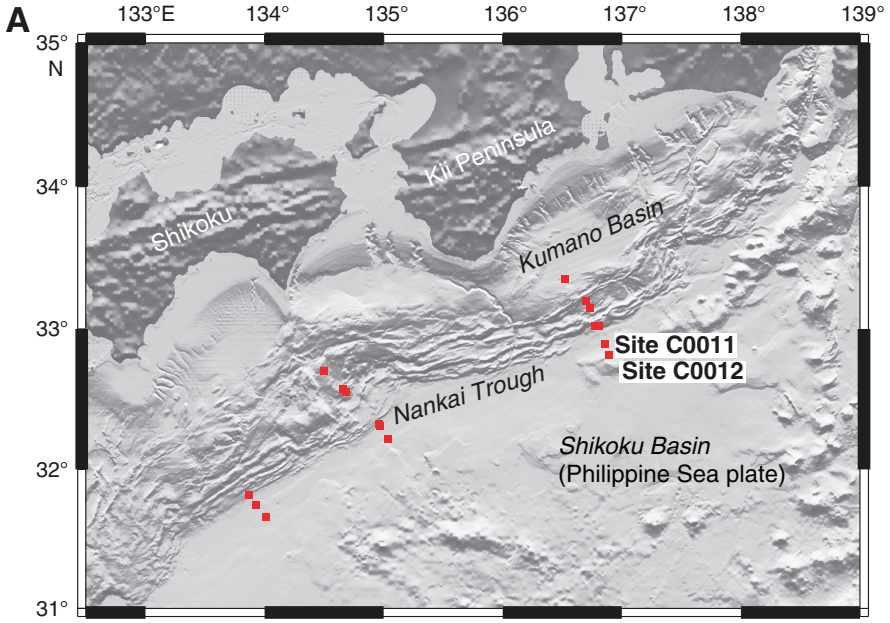

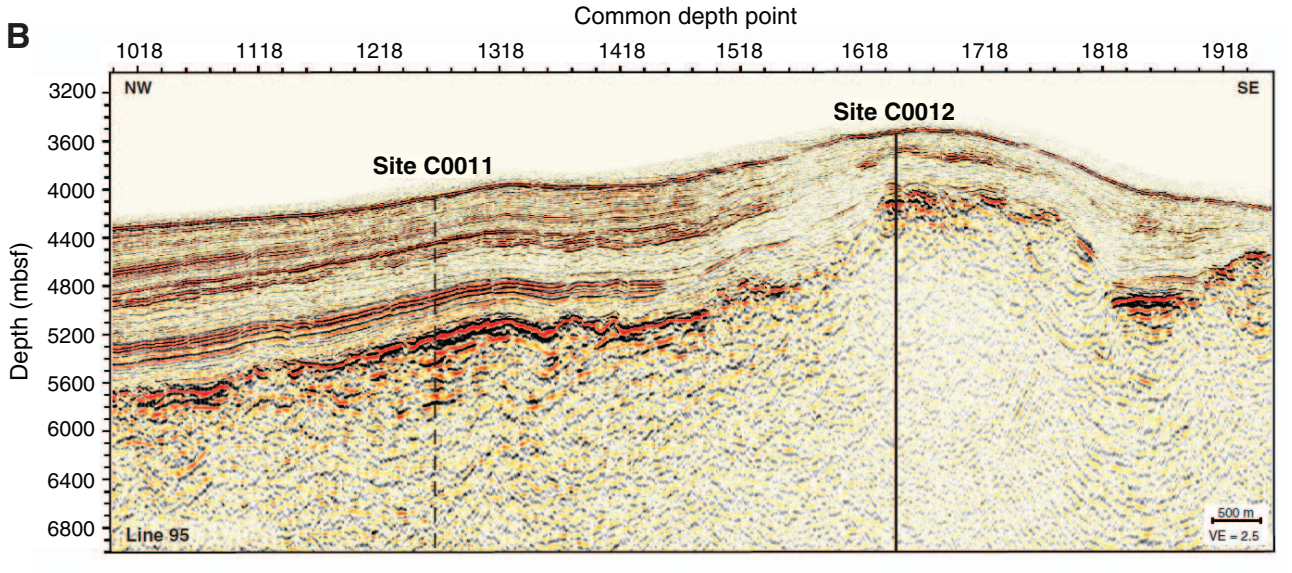

Figure F2. Downcore profiles of $^{87}Sr/^{86}Sr$ ratios in pore fluids from Sites C0011 and C0012 in the context of the sediment lithology at each site (center panel). Arrows A and B mark changes in $^{87}Sr/^{86}Sr$ ratios, which correspond to the bases of lithologic Units I and IV, respectively. Red rectangles on the *x*-axis indicate the $^{87}Sr/^{86}Sr$ ratio in modern seawater. (Lithology columns are modified from Expedition 333 Scientists, 2012.)

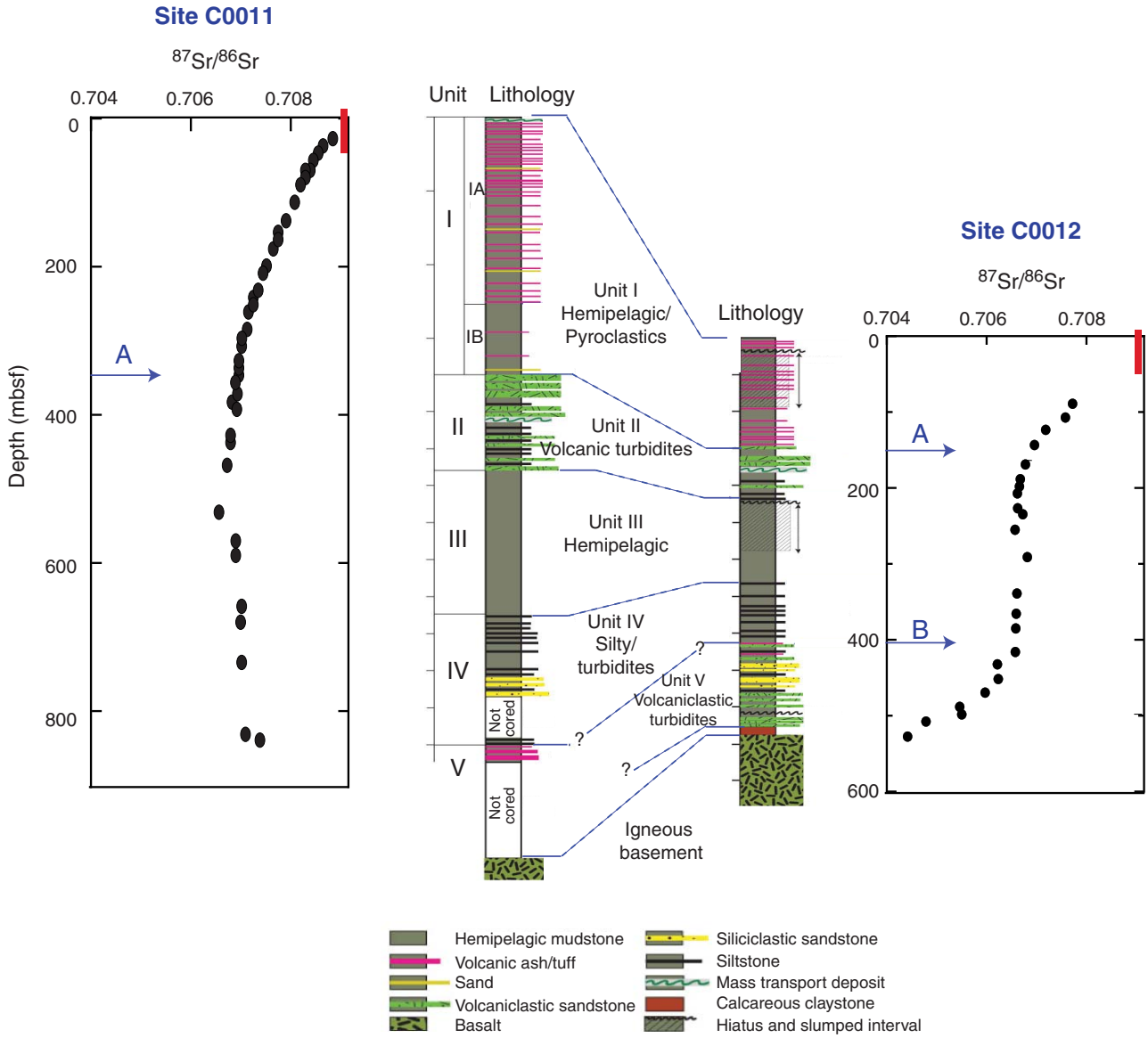

Figure F3. Relationship between the $^{87}Sr/^{86}Sr$ ratios and the inverse of the Sr concentration measured in pore fluids from Sites C0011 and C0012. Sr concentration data are from the **"Expedition 322 summary"** chapter (Underwood et al., 2010) and Expedition 333 Scientists (2012). VA = volcanic ash, OC = oceanic crust, SW = seawater value.

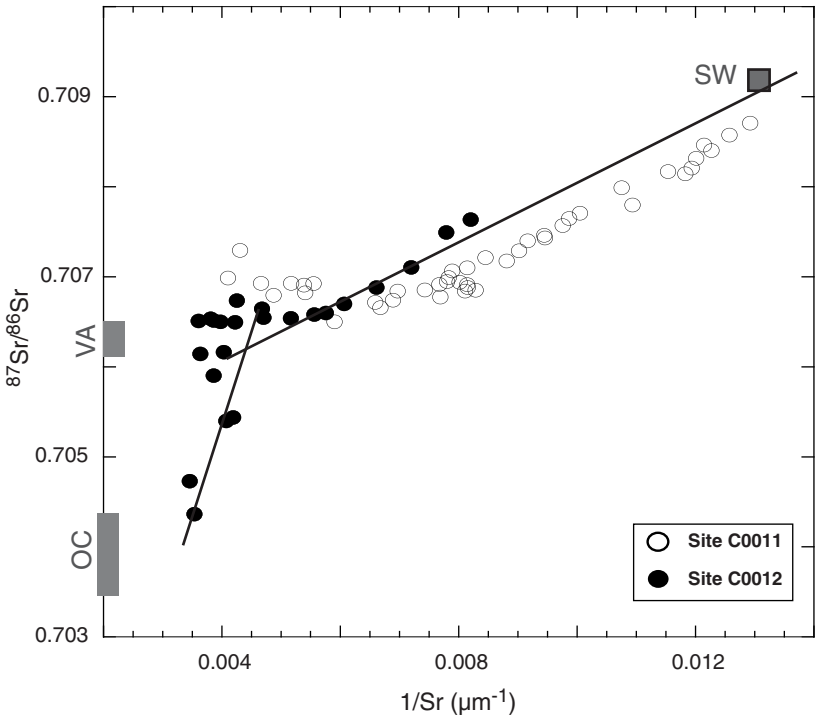

Table T1. Isotopic composition of Sr measured in pore fluid samples, Sites C0011 and C0012.

Core, section	Depth (mbsf)	$^{87}Sr/^{86}Sr$	Sr (μM)	1/Sr
333-C0011D-				
1H-4	24.98	0.708710	77	0.0129
2H-5	35.79	0.708578	80	0.0126
3H-5	44.80	0.708468	82	0.0121
4H-5	51.93	0.708406	82	0.0123
5H-5	60.69	0.708320	83	0.0120
6H-4	68.80	0.708211	84	0.0119
7H-4	76.47	0.708173	87	0.0115
9H-3	84.29	0.708148	85	0.0118
12H-5	114.25	0.707992	93	0.0107
15H-4	137.52	0.707802	91	0.0109
17H-6	154.83	0.707710	100	0.0100
18H-4	161.38	0.707650	101	0.0099
20H-4	177.81	0.707573	103	0.0098
25T-2	200.86	0.707464	106	0.0094
26X-3	206.70	0.707434	106	0.0094
27X-3	212.14	0.707404	109	0.0092
31X-4	238.14	0.707293	111	0.0090
33X-3	248.87	0.707180	114	0.0088
34X-4	254.44	0.707215	118	0.0084
36x-5	270.97	0.707103	123	0.0081
38X-3	285.32	0.707070	127	0.0079
39X-5	297.04	0.706996	128	0.0078
40X-5	306.26	0.706942	125	0.0080
41X-5	316.37	0.706950	128	0.0078
43X-3	331.80	0.706919	130	0.0077
45X-3	342.08	0.706886	123	0.0081
48X-3	356.49	0.706916	123	0.0081
49X-3	361.82	0.706844	123	0.0081
52X-4	378.56	0.706855	121	0.0083
322-C0011B-				
4R-3	366.94	0.706856	135	0.0074
6R-5	388.43	0.706777	130	0.0077
7R-3	395.13	0.706844	144	0.0070
11R-4	434.64	0.706721	152	0.0066
12R-6	446.96	0.706743	145	0.0069
16R-2	478.21	0.706661	150	0.0067
25R-2	539.86	0.706504	170	0.0059
30R-2	581.78	0.706824	185	0.0054
32R-5	601.39	0.706797	205	0.0049
40R-3	674.82	0.706928	180	0.0055
44R-3	691.09	0.706912	186	0.0054
51R-4	750.75	0.706929	215	0.0047
55R-2	779.50	0.706931	194	0.0052
57R-4	850.44	0.706991	244	0.0041
58R-3	858.34	0.707298	232	0.0043
322-C0012A-				
5R-2	89.43	0.707640	122	0.0082
7R-5	107.66	0.707497	128	0.0078
9R-04	124.03	0.707107	139	0.0072
11R-4	144.03	0.706884	151	0.0066
14R-2	169.69	0.706703	165	0.0061
16R-3	189.03	0.706601	174	0.0057
17R-3	198.82	0.706585	180	0.0056
18R-2	207.90	0.706542	194	0.0052
20R-3	227.50	0.706550	213	0.0047
23R-3	256.10	0.706499	237	0.0042
32R-2	340.13	0.706537	263	0.0038
35R-2	366.81	0.706519	259	0.0039
37R-2	386.30	0.706514	278	0.0036
40R-4	417.40	0.706502	252	0.0040
42R-2	433.90	0.706148	276	0.0036
44R-2	453.30	0.706166	248	0.0040
46R-2	471.30	0.705906	259	0.0039
48R-1	490.00	0.705402	246	0.0041
49R-2	499.90	0.705442	239	0.0042
50R-2	509.30	0.704733	290	0.0034
52R-2	529.20	0.704367	283	0.0035